340

Acta Metallurgica, Vol. 25, pp. 839–846. Pergamon Press, 1977. Printed in Great Britain

INFLUENCE OF STRAIN-RATE SENSITIVITY ON NECKING UNDER UNIAXIAL TENSION

J. W. HUTCHINSON
Division of Engineering and Applied Physics, Harvard University, Cambridge, MA 02138, U.S.A.

and

K. W. NEALE
Department of Civil Engineering, University of Sherbrooke, Sherbrooke, Quebec, Canada

(*Received* 26 *January* 1977)

Abstract—The influence of material strain-rate dependence on necking retardation is studied. A relatively small amount of strain-rate dependence is known to lead to substantially increased straining prior to necking. Criteria based on linearized stability analyses do not reveal this behavior. A nonlinear analysis for long-wavelength nonuniformities does reproduce the essential details of the phenomenon. Limitations of the analysis are discussed.

Résumé—On étudie l'influence de la variation de la vitesse de déformation sur le retard à la striction. On sait qu'une sensibilité à la vitesse de déformation relativement faible conduit à une augmentation de la déformation avant la striction. Les critères qui reposent sur des analyses linéarisées de la stabilité ne rendent pas compte de ce comportement. Une analyse non linéaire des hétérogénéités de grande longueur d'onde permet par contre de reproduire les traits principaux de ce phénomène. On discute les limitations de cette analyse.

Zusammenfassung—Es wird der Einfluß der Dehngeschwindigkeitsabhängigkeit eines Materials auf die Verzögerung der Einschnürung untersucht. Es ist bekannt, daß eine relativ kleine Dehngeschwindigkeitsabhängigkeit zu beträchtlich vergrößerter Dehnung vor der Einschnürung führt. Auf linearisierten Stabilitätsanalysen aufbauende Kriterien zeigen dieses Verhalten nicht. Eine nichtlineare Analyse für langwellige Ungleichmäßigkeiten ergibt aber die wesentlichen Einzelheiten der Erscheinung. Die Grenzen der Analyse werden diskutiert.

1. INTRODUCTION

Among the factors which influence necking or strain-localization in metals under tension are the work-hardening properties of the material and its strain-rate characteristics. For a simple bar under axial tension, the well-known construction of Considère [1] gives a reasonably good estimate of the critical strain for the onset of necking if the material is strain-rate insensitive. However, when the material response is strain-rate sensitive, a considerable delay in necking may occur [2–4]. This behavior is particularly evident for the so-called "superplastic" materials [5].

Figure 1, taken from Ghosh [3], collects together data from tensile tests on flat strip specimens of a number of metals with small, but varying, degrees of strain-rate dependence. Each data point represents the amount of overall strain attained in a test beyond maximum load (post-uniform elongation) plotted against a strain-rate sensitivity parameter m which will be introduced in a later section. It is this strong dependence on relatively small strain-rate sensitivity which is studied in this paper. We start by discussing the implications of the several *linearized* stability analyses existing in the literature. Criteria based on these linearized analyses completely miss the phenomenon illustrated by Fig. 1. It is argued that the behavior is inherently nonlinear and a relatively simple, approximate nonlinear analysis is carried out for bars

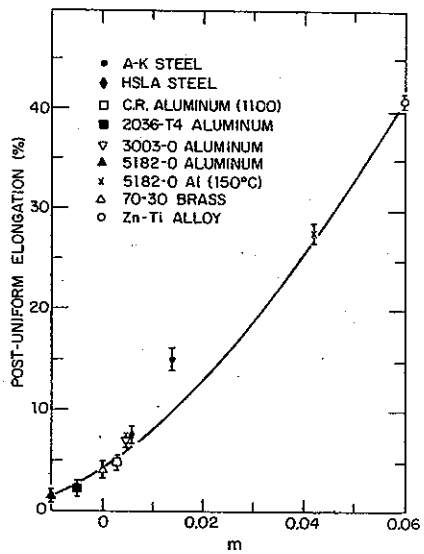

Fig. 1. Collected data by Ghosh [3] showing relation between delay in necking and strain-rate index m.

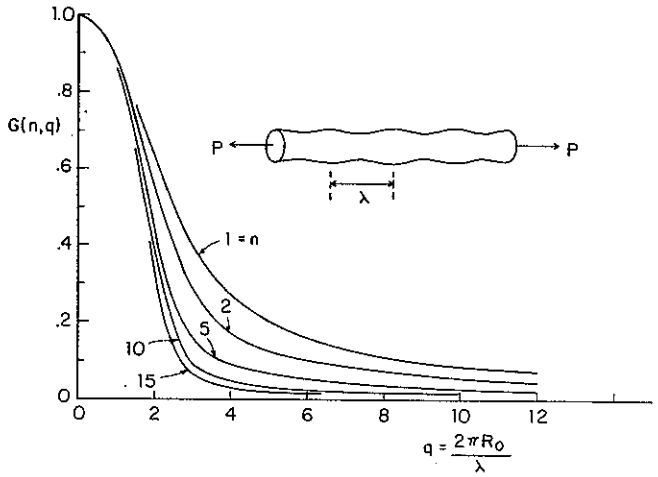

Fig. 2. Values of $G(n,q)$ in (2.7).

in tension which does reproduce the essence of the phenomenon. Results are also presented covering essentially the entire range of material parameters, including a comparison with data on the effect of large amounts of strain-rate dependence on total elongation prior to necking.

2. DISCUSSION OF STUDIES BASED ON LINEARIZED ANALYSES*

As background to discussing the linearized analyses of the type employed by Hart [6], Campbell [7], Jonas *et al.* [8] and Argon [9], we first briefly summarize some details of an exact, linearized three-dimensional solution for power law creeping materials.

Consider an infinitely long axisymmetric bar whose current cross-sectional area varies along its axis z according to

$$A = A_0[1 - \eta \cos(2\pi z/\lambda)], \tag{2.1}$$

as depicted in the insert of Fig. 2. The bar material is taken to be incompressible and nonlinearly viscous such that in simple tension the relation between the (natural) strain-rate and (true) stress is $\dot{\epsilon} = \alpha\sigma^n$. Under a multi-axial true stress state σ_{ij} the strain-rate is taken as

$$\dot{\epsilon}_{ij} = \tfrac{3}{2}\alpha\sigma_e^{n-1}s_{ij},\ \sigma_e = (\tfrac{3}{2}s_{ij}s_{ij})^{1/2}, \tag{2.2}$$

where s_{ij} is the stress deviator and σ_e is the effective stress.

In [10], the linearized problem for the stresses and strain-rates in the slightly nonuniform bar (i.e. $|\eta| \ll 1$) under load P is solved exactly. Of primary interest here is the result for the rate of growth of the relative size of the nonuniformity of cross-sectional area. Let $A_0(t)$ denote the evolving cross-sectional area of the perfect bar, $\eta = 0$, and let $A(t,z)$ be the area of the nonuniform bar at z. Define the nonuniformity in area as

$$\Delta A(t,z) = A(t,z) - A_0(t). \tag{2.3}$$

Define the measure a of the size of the nonuniformity relative to the evolving cross-sectional area of the perfect bar as

$$a(t,z) = \Delta A(t,z)/A_0(t). \tag{2.4}$$

From (2.1), the current a is taken as

$$a = -\eta \cos(2\pi z/\lambda). \tag{2.5}$$

The result of the analysis of [10] for the rate of change of a can be expressed as

$$\dot{a} = -\eta n\dot{\epsilon}_0\, G(n,q) \cos(2\pi z/\lambda), \tag{2.6}$$

or, from (2.5), as

$$\dot{a} = n\dot{\epsilon}_0\, G(n,q)a. \tag{2.7}$$

Here

$$\dot{\epsilon}_0 = \alpha(P/A_0)^n \tag{2.8}$$

is the strain-rate of the perfect bar and

$$q = 2\pi R_0/\lambda, \tag{2.9}$$

where R_0 is the radius of the perfect bar. Curves of G as a function of q for various n are shown in Fig. 2.† For small q,

$$G(n,q) = 1 - \frac{1}{8}q^2 - \frac{1}{876}\frac{1}{n}(n^2 + 3n - 9)q^4 + \cdots. \tag{2.10}$$

The limit of (2.7) for long-wavelength nonuniformities, $q \to 0$, is

$$\dot{a} = n\dot{\epsilon}_0 a. \tag{2.11}$$

This limiting result is precisely the result obtained by assuming the stress over each cross-section is uniaxial and uniform with resultant P. This assumption is often invoked in the analysis of the growth of

* This section is abstracted from [10].

† The results here are presented in a slightly different form from [10]. There, values of $f(n,q)$ were given where $\Delta\dot{A} = (n-1)\dot{\epsilon}_0 f A$. Using (2.19), this expression can be transformed to (2.7) where $nG = (n-1)f + 1$.

nonuniformities in tensile bars and will be referred to here as the *long-wavelength approximation*. From (2.7) and Fig. 2 it is clear that the relative size of the nonuniformity, a, always increases for the viscous material (2.2), albeit possibly very slowly. If $q < 1$, i.e. if $\lambda > 2\pi R_0$, the long-wavelength approximation (2.11) is reasonably accurate. Since G is a monotonically decreasing function of q for each n, the long-wavelength nonuniformity characterized by (2.11) has the fastest growth-rate.

Linearized, long-wavelength analyses have been carried out for more general materials by a number of authors [6–9]. As an illustration, consider axisymmetric bars of incompressible materials characterized in simple tension by

$$\sigma = F(\epsilon, \dot{\epsilon}), \tag{2.12}$$

where σ is the true stress, ϵ is the natural strain and a dot denotes time rate of change. The bar is subject to a load history $P(t)$. It is considered to be long compared to its single long-wavelength nonuniformity, as depicted in Fig. 3. Far from the nonuniformity, the bar is assumed to be essentially uniform with cross-sectional area $A_0(t)$. [Equivalently, $A_0(t)$ can be regarded as the area of the perfect bar under the same load history.] Denote the area of the smallest cross-section in the nonuniform region by $A(t)$ and let

$$\Delta A(t) = A(t) - A_0(t). \tag{2.13}$$

Let η measure the initial fractional nonuniformity in area according to

$$\eta = -\Delta A(0)/A_0(0), \tag{2.14}$$

where $\eta > 0$ since we will take $\Delta A(0) < 0$.

Denote by a subscript or superscript 0 all quantities associated with behavior in the essentially uniform sections far from the nonuniformity or, equivalently, with behavior in the perfect bar. The long-wavelength approximation of a uniform, uniaxial stress state over each cross-section is now invoked. Linearization about the solution for the uniform bar under the assumption $|\eta| \ll 1$ leads to a linear equation for the growth of ΔA of the type found by Hart [6]:

$$\Delta\dot{A} + h(t)\Delta A = (\gamma/m)\dot{A}_0\eta, \tag{2.15}$$

where

$$\gamma(t) = (\partial F/\partial\epsilon)_0\,\sigma_0^{-1},\ m(t) = (\partial F/\partial\dot{\epsilon})_0\,\dot{\epsilon}_0/\sigma_0 \tag{2.16}$$

and

$$h(t) = (\dot{\epsilon}_0/m)[-1 + \gamma + m]. \tag{2.17}$$

The partial derivatives in (2.16) are functions of t and are to be evaluated at $\epsilon_0(t)$ and $\dot{\epsilon}_0(t)$. Hart [6] does not explicitly incorporate the initial imperfection η into his analysis, so his equation does not include the non-homogeneous term in (2.15)—see [10] for the derivation of (2.15).

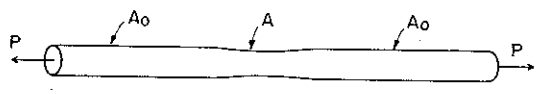

Fig. 3. Geometry of imperfect bar.

It is revealing to cast (2.15) into a different form involving the *relative* size of the nonuniformity

$$a(t) = \Delta A(t)/A_0(t). \tag{2.18}$$

Since

$$\dot{a} = \Delta\dot{A}/A_0 - \Delta A\dot{A}_0/A_0^2 = a(\Delta\dot{A}/\Delta A + \dot{\epsilon}_0), \tag{2.19}$$

equation (2.15) can be written as

$$\dot{a} + \tilde{h}(t)a = -(\gamma/m)\dot{\epsilon}_0\eta, \tag{2.20}$$

where

$$\tilde{h}(t) = (\dot{\epsilon}_0/m)[-1 + \gamma]. \tag{2.21}$$

Using the absolute size ΔA as the measure of the nonuniformity, Hart [6] notes that a positive value of h, i.e. assuming $m > 0$,

$$-1 + \gamma + m > 0 \tag{2.22}$$

implies that the homogeneous solution to (2.15) for ΔA is associated with exponential decay. Hart defines a state in which (2.22) is satisfied as being stable. Other authors prefer to measure the nonuniformity using its relative size a. Indeed, when large straining occurs prior to necking, as in the tests of Sagat and Taplin [5] discussed below, the relative size a is clearly a more meaningful measure than ΔA. From (2.20), exponential decay of the homogeneous solution for a requires $\tilde{h} > 0$, i.e.

$$-1 + \gamma > 0. \tag{2.23}$$

Condition (2.23) is favored over (2.22) as a stability criterion by Jonas *et al.* [8]. They use the difference between the axial strain at the narrowest cross-section and that away from the nonuniformity, $\Delta\epsilon = \epsilon - \epsilon_0$, as their measure of nonuniformity. But it is readily shown that in the long-wavelength approximation $\Delta\dot{\epsilon} = -\dot{a}$, and thus a criterion based on growth or decay of $\Delta\epsilon$ is identical to that based on a, i.e. (2.23).

It has been suggested that a transition from $h > 0$ to $h < 0$ (or from $\tilde{h} > 0$ to $\tilde{h} < 0$) could be used as a criterion to predict the effect of strain-rate dependence on tensile instabilities. Recent work indicates that neither criterion is useful for this purpose. In addition to the data of Fig. 1, which will be mentioned again in the next section, Sagat and Taplin [5] conducted uniaxial necking tests on a class of metals with strong strain-rate dependence (m being as large as 0.4). They found that the transition criterion $h = 0$ predicted overall strains at necking which were not even qualitatively correct. For example, in one case in which experimentally measured values of m and γ implied that h became negative at an axial strain of about 0.02, nonuniformities could not be detected by eye until strains of about 0.7 were attained. That such behavior should be expected is actually apparent

from either (2.15) or (2.20), as noted in [10]. Since the magnitude of h (or $\tilde{h}$) is proportional to $\dot{\epsilon}_0$, the characteristic time for exponential growth will be on the order of the time scale associated with development of strains of order unity in the uniform sections of the bar if m is not small. In other words, even if $h < 0$ (or $\tilde{h} < 0$), the rate of exponential growth can be exceedingly slow, and a sign change of h or $\tilde{h}$ positive to negative has no immediate significance as far as observable behavior is concerned.

Nonlinearity, whether it be geometric, material or both, is inherently a part of the necking process. While linear analyses such as those discussed above can provide the very early development of small nonuniformities, it appears they cannot be used to estimate the influence of imperfections or material parameters on rupture times or on the amount of attainable strain.

3. NONLINEAR LONG-WAVELENGTH ANALYSIS

As emphasized in the previous section, it is essential that nonlinearities be properly accounted for in an analysis of the necking process. Here, a nonlinear analysis based on the long-wavelength approximation referred to above is applied to study the growth of geometric nonuniformities in a strain-rate sensitive material. The approach is essentially a one-dimensional version of the analysis introduced by Marciniak and Kuczyński [11, 12]. We consider a long cylindrical solid bar (Fig. 3) subjected to a time-dependent axial load $P(t)$, and examine the growth of the nonuniformity $\Delta A(t) = A(t) - A_0(t)$. As previously indicated, $A(t)$ denotes the area at time t of the cross-section where necking eventually occurs, and $A_0(t)$ refers to the corresponding area in the uniform sections or of the perfect bar.

According to the long-wavelength simplification

$$\sigma = \frac{P}{A}, \sigma_0 = \frac{P}{A_0} \tag{3.1}$$

represent the values of true stress at the "local" section A and "uniform" section A_0, respectively. Furthermore, for an incompressible material, the conventional definition of natural or logarithmic strain gives

$$\epsilon = -\ln \frac{A}{A(0)}, \epsilon_0 = -\ln \frac{A_0}{A_0(0)} \tag{3.2}$$

and

$$\dot{\epsilon} = -\frac{\dot{A}}{A}, \dot{\epsilon}_0 = -\frac{\dot{A}_0}{A_0}. \tag{3.3}$$

As a result of (3.2), the relative nonuniformity introduced in (2.18) is given by

$$a(t) = \frac{\Delta A(t)}{A_0(t)} = (1-\eta)\exp(\epsilon_0 - \epsilon) - 1, \tag{3.4}$$

where η is the initial geometric nonuniformity defined by (2.14). It is clear from the above relation that the relative values of the "local" strain $\epsilon(t)$ and the "uniform" strain $\epsilon_0(t)$ also provide an adequate measure of geometric nonuniformity. Since we shall be primarily interested in the amount of strain, ϵ_0, attainable in the uniform sections, we shall therefore work with the growth of ϵ and ϵ_0 in the following and identify the critical state for necking in terms of the relative values of these quantities. A more precise definition of this critical condition will be given shortly.

Although three-dimensional effects are obviously being neglected here, it might be argued that the long-wavelength approximation will under-estimate the actual total elongation of the bar required for necking. For example, a Bridgman-type analysis [13] for the three-dimensional stress state in a neck under time-independent plastic conditions indicates that the effective stress there would be less than the average stress σ given by (3.1). This implies that the actual strain in the neck is also less than the strain ϵ calculated in the present analysis. Thus, necking proceeds more rapidly when the long-wavelength simplification is invoked and the critical state should be attained earlier than in an analysis where three-dimensional effects are included.

To describe time-dependent material response under uniaxial tension, the following constitutive law [3, 4] will first be employed

$$\sigma = K\epsilon^N\dot{\epsilon}^m, \sigma_0 = K\epsilon_0^N\dot{\epsilon}_0^m. \tag{3.5}$$

Here K is a constant, and N and m denote the strain hardening and strain-rate hardening exponents, respectively. The parameters P and K can now be readily eliminated from (3.1) and (3.5). This, together with (3.2) and (2.14), furnishes the desired relationship between the increments (or rates) of local and uniform strain:

$$e^{-s\epsilon}\epsilon^p\, d\epsilon = \frac{1}{(1-\eta)^s} e^{-s\epsilon_0}\epsilon_0^p\, d\epsilon_0, \tag{3.6}$$

in which $p = N/m$ and $s = 1/m$. With initial conditions $\epsilon(0) = \epsilon_0(0) = 0$, the integrated form of (3.6) becomes

$$\int_0^{\epsilon} e^{-st}t^p\, dt = \frac{1}{(1-\eta)^s}\int_0^{\epsilon_0} e^{-st}t^p\, dt. \tag{3.7}$$

This result brings out an interesting feature of our analysis, namely that the relationship between ϵ and ϵ_0 is independent of the load history $P(t)$ experienced by the bar and, in particular, is independent of the rate at which the bar is being deformed.

For time-independent material behavior ($m = 0$), the long-wavelength analysis presented above gives

$$e^{-\epsilon}\epsilon^N = \frac{1}{(1-\eta)} e^{-\epsilon_0}\epsilon_0^N. \tag{3.8}$$

The above expressions (3.7) and (3.8) were applied to some specific examples in order to illustrate the strain-localization process in the bar and to assess the influence of strain-rate sensitivity. Typical results are shown in Fig. 4, where curves of ϵ/ϵ_0 are plotted

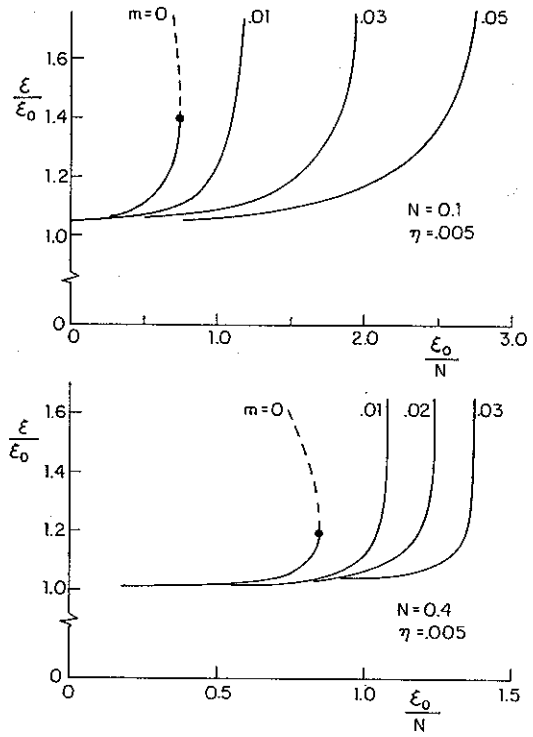

Fig. 4. Ratio of strain at necking region to strain in uniform section as a function of normalized strain in uniform section.

against the normalized uniform strain ϵ_0/N for an initial geometric nonuniformity $\eta = 0.005$.

For the case $m = 0$, the curves of Fig. 4 were determined from a direct numerical solution of the transcendental relation (3.8). The solid dots on these curves indicate the maximum value of ϵ_0, which, in view of (3.8), is given by

$$\frac{\bar{\epsilon}_0^c}{N}\exp - \left(\frac{\bar{\epsilon}_0^c}{N} - 1\right) = (1 - \eta)^{1/N}. \tag{3.9}$$

This occurs when the local strain satisfies $\epsilon = N$ and the corresponding load on the specimen reaches a maximum. The dashed portion of the curve is also obtained from (3.8), but is no longer valid since unloading occurs in the uniform sections. The important point, however, is that $\bar{\epsilon}_0^c$ given by (3.9) is the maximum value of the strain attained in the uniform sections. Note that the classical result for time-independent behavior, $\bar{\epsilon}_0^c = N$, is retrieved from (3.9) when $\eta = 0$.

For the case $m \neq 0$, the curves of Fig. 4 were determined by integrating (3.7) in a straightforward incremental fashion. It can be seen from these results that a very small nonuniformity grows slowly from the onset of loading, but that extremely rapid growth or localization eventually occurs. The value of ϵ_0 also attains a maximum for this case; however, in contrast to the response when $m = 0$, the uniform strain ϵ_0 now reaches a maximum when $\epsilon \to \infty$.

The above results suggest that instability be identified with ϵ_0^c, the maximum value of ϵ_0. Consequently, we define the critical state for necking as that for which $d\epsilon_0/d\epsilon = 0$. This provides a unified criterion for both time-dependent and time-independent behavior; but we will use the special symbol $\bar{\epsilon}_0^c$ to denote the value of ϵ_0^c for $m = 0$. For time-dependent material behavior ($m \neq 0$), the critical value ϵ_0^c is obtained by inserting the limits $\epsilon_0 = \epsilon_0^c$ and $\epsilon = \infty$ in the integral (3.7). It is perhaps interesting to note that, for integer values of p, (3.7) can be integrated analytically and that the above stability criterion furnishes the following expression for the critical strain ϵ_0^c:

$$\exp(-s\epsilon_0^c)\sum_{k=0}^{p}\frac{(s\epsilon_0^c)^k}{k!} = [1 - (1 - \eta)^s]. \tag{3.10}$$

We emphasize again that the present analysis is concerned mainly with the strain parameter ϵ_0^c. In a finite length test specimen, however, it is the *combined* contributions from ϵ_0 and ϵ which produce the total elongation. Consequently, the distinction between ϵ_0 and a measured overall average axial strain must be properly accounted for in any correlation with test data.

The curves of Fig. 4 clearly indicate that time-dependent effects greatly influence the strain ϵ_0^c that can be achieved prior to necking. Figure 5 illustrates the delay in necking for small values of strain-rate exponent ($m \leq 0.05$). Here,

$$\delta\epsilon = \epsilon_0^c - \bar{\epsilon}_0^c \tag{3.11}$$

is the increase due to strain-rate dependence of the maximum strain attainable in the uniform sections above the corresponding strain for the time-independent material ($m = 0$). Very small values of m lead

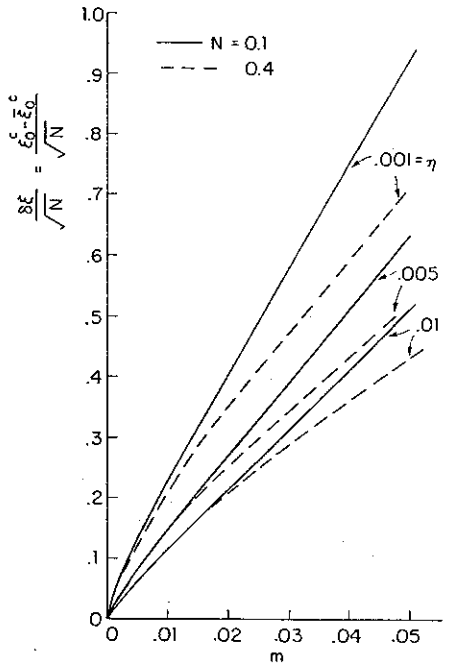

Fig. 5. Additional maximum strains in uniform sections as a function of strain-rate index m.

to relatively large increases in ϵ_0^c, similar to the trend of Ghosh's plot for thin strips in Fig. 1. It is also evident that $\delta\epsilon$ decreases with increasing initial nonuniformity η, and increases with increasing strain-hardening exponent N. In fact, the numerical results depicted in Fig. 5 indicate that $\delta\epsilon$ is nearly proportional to $\sqrt{N}$ for small m, as suggested by the asymptotic analysis discussed in the next section.

The above analysis, which is based on the constitutive law (3.5), leads to the interesting conclusion that ϵ_0^c is determined solely by the parameters m, η and N. Thus, according to this model, the strain rate $\dot{\epsilon}_0$ experienced by the bar has no effect on the eventual necking strain. This conclusion is not exactly true, however, for an alternative constitutive law recently proposed by Ghosh [4]:

$$\sigma = K\left[\epsilon^N + m \ln\left(\frac{\dot{\epsilon}}{\dot{\epsilon}_r}\right)\right]. \tag{3.12}$$

Here, N and m again represent strain hardening and strain-rate hardening constants, respectively, and the additional parameter $\dot{\epsilon}_r$ is a reference strain-rate. When this law is employed in the previous long-wavelength analysis, the following expression, analogous to (3.6), is obtained

$$\ln\left(\frac{\dot{\epsilon}}{\dot{\epsilon}_r}\right) = \frac{\exp(\epsilon - \epsilon_0)}{(1-\eta)}\left[\frac{\epsilon_0^N}{m} + \ln\left(\frac{\dot{\epsilon}_0}{\dot{\epsilon}_r}\right)\right] - \frac{\epsilon^N}{m}, \tag{3.13}$$

in which the strain-rate is inherently present. Here, again, the critical strain ϵ_0^c for which $d\epsilon_0/d\epsilon = 0$ occurs when $\epsilon \to \infty$. A straightforward incremental technique was employed to numerically solve (3.13) for the critical strain ϵ_0^c for the case $N = 0.1$, $\eta = 0.005$ and various values of m and imposed strain-rate $\dot{\epsilon}_0$. The results of these calculations are shown in Fig. 6 where they are compared with those obtained previously using the law (3.5). Very little difference between the predictions of both laws can be observed. Furthermore, although there is some dependence on $\dot{\epsilon}_0$ with Ghosh's constitutive law, it can be seen that an increase in the imposed strain-rate by a factor of 4 has only a very minor effect on ϵ_0^c.

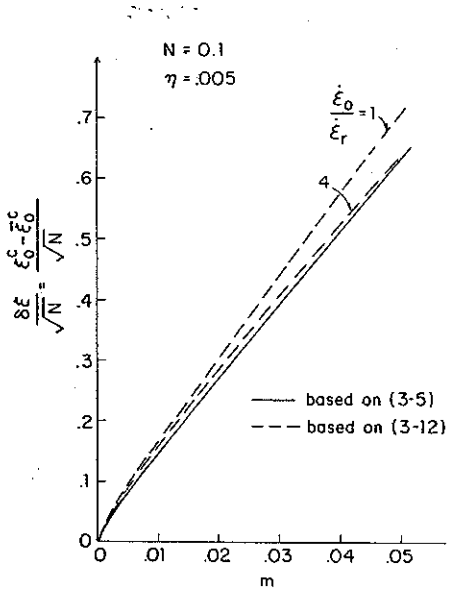

Fig. 6. Comparison of the additional maximum strains in uniform sections for two uniaxial constitutive laws.

In contrast to the results of the nonlinear long wavelength analysis just discussed, predictions based on the criterion $h = 0$ (or $\tilde{h} = 0$) derived from the linearized analyses indicate no strong dependence of ϵ_0^c on m. For example, using (2.16) and (2.17) and the law (3.5) one finds that h changes sign from positive to negative, implying loss of stability according to [6], when

$$\epsilon_0 = N/(1-m).$$

Not only does this result fail to reveal any dependence on η, it implies a weak strain-rate effect compared to the results of either Figs. 1 or 5. The analogous prediction based on (2.21) gives $\epsilon_0 = N$ when $\tilde{h}$ becomes negative, implying no strain-rate dependence.

4. ASYMPTOTIC ANALYSIS FOR THE EFFECT OF SMALL m

The numerical results of the previous section indicate that very small values of the strain-rate exponent m can substantially increase the strain ϵ_0^c beyond its time-independent value $\bar{\epsilon}_0^c$. This suggests that an asymptotic expansion about $\bar{\epsilon}_0^c$ might be carried out to determine an approximate relation for the influence of small m on ϵ_0^c. Such an analysis is performed in this section for the case where the material response is described by (3.5). The approach consists of applying Laplace's method [14] to obtain approximate expressions for the integrals (3.7). We note first, however, that in the time-independent case ($m = 0$) an asymptotic expansion of $\bar{\epsilon}_0^c$ about N for small η using (3.9) gives

$$\frac{\bar{\epsilon}_0^c}{N} \simeq 1 - \sqrt{\frac{2\eta}{N}}. \tag{4.1}$$

As discussed previously, the criterion introduced in the present analysis implies that $\epsilon \to \infty$ as the critical strain ϵ_0^c is attained. Consequently, from (3.7)

$$\int_0^\infty \exp[-sg(t)]\,dt = \frac{1}{(1-\eta)^s}\int_0^{\epsilon_0^c} \exp[-sg(t)]\,dt \tag{4.2}$$

determines ϵ_0^c, where

$$g(t) = t - N \ln t. \tag{4.3}$$

Consider first the integral on the left of the equal sign in (4.2). Since $g(t)$ has a minimum on the interval $0 < t < \infty$ at $t = N$, when $s(= 1/m)$ is large, the major contribution to the integral is from the neighborhood of $t = N$. A straightforward application

of Laplace's method gives

$$\int_0^\infty \exp[-sg(t)]\,dt \cong \exp[-Ns(1-\ln N)] \times [2\pi N/s]^{1/2}. \quad (4.4)$$

Next, to evaluate the other integral in (4.2) it must be noted that as $m \to 0$, $\epsilon_0^c \to \bar{\epsilon}_0^c$, which is less than N when $\eta > 0$ from (4.1). Therefore, for sufficiently small m, the point $t = N$ where $g' = 0$ lies outside the range of integration $0 \le t \le \epsilon_0^c$. In this case, for large s, the major contribution to the integral comes from the neighborhood of ϵ_0^c. Applying Laplace's method here gives

$$\int_0^{\epsilon_0^c} \exp[-sg(t)]\,dt \simeq \left[s\left(\frac{N}{\epsilon_0^c}-1\right)\right]^{-1} \times \exp[-s(\epsilon_0^c - N\ln\epsilon_0^c) \quad (4.5)$$

valid for large s and $\epsilon_0^c < N$.

When the above asymptotic approximations are substituted into (4.2), an explicit algebraic expression relating ϵ_0^c, m, η and N is obtained. As $m \to 0$, this expression reduces to the time-independent result (3.9) for $\bar{\epsilon}_0^c$. Thus with

$$\epsilon_0^c = \bar{\epsilon}_0^c + \delta\epsilon, \quad (4.6)$$

an asymptotic expression for $\delta\epsilon$ in terms of large s (small m) can be obtained. The result is

$$\frac{\delta\epsilon}{\sqrt{N}} \simeq \frac{m}{2\sqrt{2\eta}}\ln\left(\frac{4\pi\eta}{m}\right). \quad (4.7)$$

In deriving (4.7), the relation (4.1) is used so that it is assumed that $\eta \ll 1$. Furthermore, (4.7) is restricted to values of m and η satisfying $m \le 2\eta$, which ensures that ϵ_0^c is less than N. The higher-order terms neglected in the analysis indicate that m/N should be small as well.

It is the above relation (4.7) which suggested that $\delta\epsilon$ be normalized by $\sqrt{N}$ in Fig. 5. Note also that the slope of the $\delta\epsilon - m$ relation is infinite at $m = 0$, already indicating an unusually strong dependence on m.

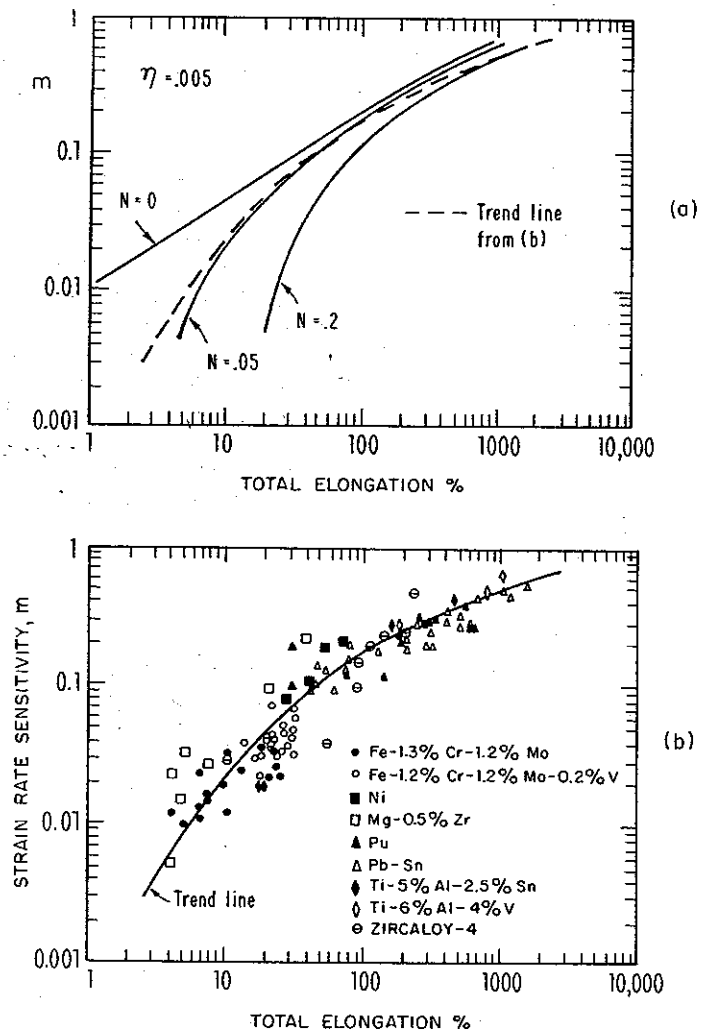

Fig. 7. (a) Relation between strain-rate index and total elongation as calculated from (3.7). (b) Collected data from Woodford [16].

5. NUMERICAL RESULTS FOR FULL RANGE OF m

Using the relation (3.7) with $\epsilon = \infty$ and $\epsilon_0 = \epsilon_0^c$, numerical results for the critical strain ϵ_0^c were generated for a wide range of material parameters m and N in the constitutive law (3.5). Typical results are shown in Fig. 7(a) where the total elongation at necking is plotted against m for $\eta = 0.005$ and $N = 0$, 0.05 and 0.2. Here, to draw comparison with previously published data in Fig. 7(b), the total elongation is measured as (percentage of) engineering strain, i.e. $\exp[(\epsilon_0^c) - 1]$. The curve corresponding to $N = 0$ was obtained from the relation

$$\epsilon_0^c = -m \ln [1 - (1 - \eta)^{1/m}], \qquad (5.1)$$

which follows immediately from (3.10) and which, when converted to engineering strain, is identical to that given by Ghosh in [3]. The results of Fig. 7(a) indicate again that the amount of strain that can be achieved prior to necking increases sharply with increasing strain-rate exponent m. From this figure it is also apparent that the value of strain-hardening exponent N is relatively unimportant for the higher values of m, but that variations in both m and N substantially affect the critical strain ϵ_0^c in the lower range of m.

In Fig. 7(b), Woodford's [16] compilation of experimental data for a variety of materials is given. The trend line from this plot is reproduced as the dashed line in Fig. 7(a), and is seen to lie in the range of numerical results predicted by the present analysis.

6. CONCLUSION

The relatively simple nonlinear long-wavelength analysis demonstrates the strong influence of a very small degree of material strain-rate dependence on retarding necking localization. It seems likely that the long-wavelength analysis actually underestimates the amount of essentially uniform straining attainable prior to necking failure. As discussed in the paper, this is due to inherently three-dimensional aspects of stress distribution which develop as necking progresses. In one form or another, the long wave approximation is invoked by many authors, but its limitations are not fully understood. The approach of Marciniak and Kuczyński [11] to necking failure in thin sheets of time-independent materials under biaxial tension involves approximations similar to those used here, as does their work [12] accounting for time-dependent material behavior in sheet necking. Burke and Nix [15] also adopt the long-wavelength approximations in their nonlinear analysis of neck development in nonlinear viscous materials of the type (2.2). Even when nonuniformities are very small three dimensional effects can be important when their wavelengths are short. For example, from (2.7) and Fig. 2, it is seen that for sinusoidal nonuniformities with wavelength λ less than πR_0 (i.e. $q > 2$) the growth-rate is a small fraction of the long wavelength growth-rate. The extent to which inherently three-dimensional features modify predictions of the long-wavelength analysis requires further investigation. An *ad hoc* approach to necking in flat strip specimens by Ghosh [4] does incorporate such features in an approximate way and allows for the possibility of numerical calculations which are not inordinately heavy. In particular, his numerical results, analogous to those in Fig. 5, appear to be in good agreement with the trend of the experimental data for strips which he collected in Fig. 1.

Acknowledgement—The work of J.W.H. was supported in part by the Air Force Office of Scientific Research under Grant AFOSR-73-2476, and by the Division of Engineering and Applied Physics, Harvard University. K.W.N. gratefully acknowledges the support of the University of Sherbrooke.

REFERENCES

1. A. Considère, *Ann. Ponts Chaussées* **9**, 574 (1885).
2. A. K. Ghosh, *Met. Trans.* **5**, 1607 (1974).
3. A. K. Ghosh, *J. Eng. Mat. Tech.* to be published (1977).
4. A. K. Ghosh, *Res. Lab. General Motors Corp.* (1976).
5. S. Sagat and D. M. R. Taplin, *Metal Sci.* **10**, 92 (1976).
6. E. W. Hart, *Acta Met.* **15**, 351 (1967).
7. J. D. Campbell, *J. Mech. Phys. Solids* **15**, 359 (1967).
8. J. J. Jonas, R. A. Holt and C. E. Coleman, *Acta Met.* **24**, 911 (1976).
9. A. S. Argon, *The Inhomogeneity of Plastic Deformation*, Chapter 7. American Society of Metals, Metals Park, Ohio (1973).
10. J. W. Hutchinson and H. Obrecht, *Proc. 4th Int. Conf. on Fracture*, Vol. **1**, p. 101. Waterloo, Canada (1977).
11. Z. Marciniak and K. Kuczyński, *Int. J. mech. Sci.* **9**, 609 (1967).
12. Z. Marciniak, K. Kuczyński and T. Pokora, *Int. J. mech. Sci.* **15**, 789 (1973).
13. P. W. Bridgman, *Studies in Large Plastic Flow and Fracture*. Harvard University Press (1964).
14. C. E. Pearson, *Handbook of Applied Mathematics*. Van Nostrand–Reinhold, New York (1974).
15. M. A. Burke and W. D. Nix, *Acta Met.* **23**, 793 (1975).
16. D. A. Woodford, *Trans. Am. Soc. Metals* **62**, 291 (1969).